Dynamic Behaviour and Sensitivity Analysis of 5 kW PEMFC Stack Simulation

Arshad Ahmad[1] Ahmad Raoof Ramli[2]

[1]*Department of Chemical Engineering*
Universiti Teknologi Malaysia, 81310 UTM Skudai, Johor, Malaysia
Tel: +60-7-553-5610, Fax: +60-7-558-1463, Email: arshad@fkkksa.utm.my

[2]*Laboratory of Process Control, Department of Chemical Engineering*
Universiti Teknologi Malaysia, 81310 UTM Skudai, Johor, Malaysia
Tel: +60-7-555 35858, Email: op_del@lycos.com

Abstract

This paper describes a three-dimensional 5 kW PEMFC stack dynamic model. Both time and spatial dependence are considered. Dynamic response and sensitivity analyses of the stack are carried out using MATLAB and Simulink modules. The results highlight the three-dimensional distributions of species concentrations, power density and temperature for the model. The effects of feed flow rates on the stack power performance are illustrated. The result confirmed that the model developed as a reasonable representation of the fuel cell stack system.

Keywords:

Three-dimensional 5 kW PEMFC stack; finite differences scheme; stack power performance.

Introduction

The use of combustion engine in automotive applications suffers from two main drawbacks. The first issue is related to pollution from the exhaust gas emission. To address this concern, substantial efforts have been carried out. For example, the design of catalytic reactors has made the automotive engine substantially cleaner during the last two decades. Automotive manufacturers have applied large efforts in reducing the emissions of hazardous gases from the combustion engine. However, it has still been proven to be difficult to eliminate NOx and SOx emissions from this process.

The second issue is regarding the overall efficiency achievable by the combustion engine. The chemical energy of gasoline is converted to mechanical energy via the production of heat in the combustion process. The efficiency of this process is limited by the efficiency formula for the Carnot cycle. This limit serves as the upper limit and hence cannot be further improved.

A more efficient process, and one of the main candidates for power production in future automotives, is the new generation of fuel cells. The cells in principal work similar as batteries, yet while batteries are essentially batch reactors, fuel cells are continuous reactors. In a fuel cell-powered engine, the chemical energy in the fuel is converted to electrical energy and then to mechanical energy by an electric motor. The process bypasses the limitations of the Carnot cycle, and the theoretical efficiency is substantially higher than that of the combustion engine as illustrated in figure 1. This implies that a fuel cell-powered automotive will be able to run for longer distance using the same amount of fuel compared to a conventional automotive. Carbon dioxide emissions are consequently lowered, since smaller amounts of fuel are consumed for the same distance travelled. The low temperatures in the process practically eliminate the production of NOx and SOx and hence should in principle be cleaner than the existing automotive engine.

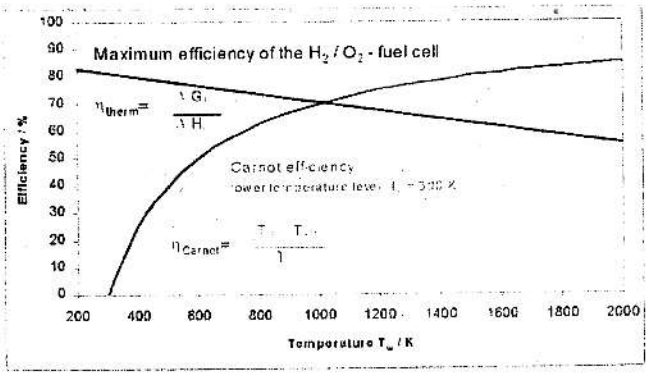

Figure 1- Thermodynamic Efficency for Fuel Cells and Carnot Efficiency for Heat Engines.

Several researchers have developed models to characterize actual PEM fuel cell operation. Springer et al. [1] reported an isothermal, one-dimensional, steady state model for complete PEM fuel cell with a 117 Nafion membrane. Their model was employed water diffusion coefficients, electro-osmotic drag coefficients, water sorption isotherms and membrane conductivities, which were measured in

ISBN:983-2643-15-5

their experiment as functions of membrane water content and equilibrium conditions between membrane liquid water and electrode water vapour at the membrane-electrode interfaces were applied. Their model also predicted an increase in membrane resistance with increased current density and showed the advantage of a thinner membrane in alleviating the resistance problem. Their model prepared the foundation for these simulations by also providing the key properties of the membrane required for a numerical model. However, they considered a pseudo one-dimensional model in which flow channels were treated as being well mixed.

Srivinivasan et al. [2] conducted studies of four PEM fuel cells: 125 μm thick Dow membrane with high platinum loading (10 mg/cm^2) electrodes and with low platinum loading (0.4 mg/cm^2) electrodes, a 100 μm thick Nafion membrane with low platinum loading and a 175 μm thick Nafion membrane with low platinum loading. Equation 2.23 was used to describe fuel cell voltage as a function of current density:

$$E = E_o - b\log(i) - Ri \qquad (1)$$

where:

E = fuel cell potential or voltage
E_o = ideal fuel cell potential
b = Tafel slope for oxygen reduction reaction
R = cell resistance (primarily ohmic and charge transfer resistance)
i = current density.

The second term on the right hand side of Equation (1) represents activation polarization effects while the third represents ohmic resistance effects. Based on experimental results, non-linear least-squares fit technique is used to determine E_o, b and R for each fuel cell analyzed.

Amphlett et al. [3 and 4] developed a steady-state model for a Ballard PEM fuel cell using a combined mechanistic and empirical approach. Using mass transport analysis, oxygen and hydrogen partial pressures and concentrations at the catalyst surfaces are determined. An expression for the actual voltage is developed based on ideal voltage at standard temperature and pressure, activation polarization as a function of temperature, current density and oxygen concentration, and ohmic polarization as a function of temperature and current density. Using experimental data from a single Ballard Mark IV PEM fuel cell, parametric coefficients for the activation polarization and ohmic polarization functions are determined. For the range of values used for temperature, oxygen partial pressure and current density, the experimental data for actual voltage agree well with the model results.

West and Fuller [5] designed two-dimensional analysis of PEM fuel cell by studying the effect of rib sizing that restrict the access of fuel and oxidant gases to the catalyst layer and the thickness of the gas-diffusion electrode on the current and water distribution within the cell. They showed the expected change in cell performance that affects from the partial blocking of the substrate layer. However, in their work they considered only the half-cell potential for a given applied current.

Lee et al. [6 and 7] developed a model for a PEM membrane/electrode assembly that can be integrated into numerical model of complete fuel cell stack. Empirical equations were used to model physical processes, polarizations and electrical characteristics. These equations are incorporated into a larger dynamic model to determine electrical performance of a fuel cell stack. The dynamic model accounts for differences in local temperature, pressure, humidity and oxygen concentration within the stack. Results from the model were reasonable in comparison to established performance experimental results.

Gurau et al. [8] included two-dimensional, non-isothermal mathematical model for a PEM fuel cell. To simulate transport phenomena and performance of PEM fuel cells, equations were developed to calculate actual concentration distributions along the interface between the gas diffuser and catalyst layer. Non-dimensional transport equations were applied to three domains: the cathode gas channel-gas diffuser-catalyst layer for the air mixture, the cathode gas diffuser-cathode catalyst layer-membrane-anode catalyst layer-anode gas diffuser for liquid water, and the anode gas channel-gas diffuser –catalyst layer for hydrogen. The transport equations were solved numerically. Results from the mathematical model were compared with previously published results based on one-dimensional numerical models. The author suggested that the results should be considered mostly qualitatively. Unlike other models, this model is able to predict phenomena in the region where concentration polarization is predominant.

Kulikovsky et al. [9] developed a two-dimensional simulation of the cathode compartment of PEM fuel cell and only investigated the influence of two-dimension effects on cathode performance. Their model was based on continuity equations for concentration of the gases and Poisson's equations for the potentials of membrane and carbon phase, coupled by Tafel relation for reaction kinetics. Their results presented that for a low value of carbon phase conductivity, a "dead zone" in the active layer in front of the gas channel is formed, where the reaction rate is small. The catalyst might be removed from this zone without significant loss in cell performance. Consequently, these results showed the possibilities for a considerable reduction of the amount of catalyst.

Djanie [10] developed a dynamic model of Proton Exchange Membrane Fuel Cell (PEMFC) plant. The plant model was derived based on information gathered in the

ISBN:983-2643-15-5

literature. Based on this model, the dynamic response of the plant was analyzed and the required control system was designed. In this plant, the fundamental theories of the PEM fuel cell were based on conservation of mass and energy. The current density was considered to be the product of the plant instead the power. Thus, the PEM fuel cell operation functions were not exactly the behaviour of the real PEM fuel cell operation. The PEM fuel cell model did not considered the effect of the ohmic loss, anode and cathode performances, Oxygen and Hydrogen concentrations distributaries within the area, the humidity of the cell and the charge transfer resistance. Furthermore, the model used many assumptions to simplify the PEM fuel cell operations due to the complex process.

Mann et al [11] developed a model to predict the steady-state performance of solid polymer electrolyte fuel cells (PEMFC). In general, the model has not been applicable to cells with different characteristics, dimensions, etc. The development of a generic model will accept as input not only values of the operating variables such as anode and cathode feed gas, pressure and compositions, cell temperature and current density, but also cell parameter including active area and membrane thickness. A further feature of the model was the addition of a term to account for membrane ageing. The resulting model was largely mechanistic, with most terms being derived from theory or including coefficients that have a theoretical basis. The major nonmechanistic term was the ohmic overvoltage that was primarily empirically based. Data for various PEM cell designs were well correlated by the model. Due to differences in the characteristics of the electocatalyst was the lack of agreement of the model predictions with some experimental results.

Rowe and Li [12] developed a one dimensional non-isothermal model of a proton exchange membrane (PEM) fuel cell. The motives of the model were to investigate the effect of various design and operating conditions on the cell performance, thermal response and water management and to understand the underlying mechanism. The model included variable membrane hydration, ternary gas mixtures for both reactant streams, phase change of the water in the electrodes with unsaturated reactant gas streams and the energy equation for the temperature distribution across the cell. The temperature distribution within the PEM fuel cell was found to be affected by water phase change in the electrodes, especially for unsaturated reactant streams. Larger peak temperatures occurred within the cell at lower cell operating temperatures and for partially humidified reactants as a result of increased membrane resistance arising from reduced membrane hydration. The results of the model indicated that operating temperature and pressure can be optimized, based on cell performance, for given design and other operating conditions.

Djilali and Lu [13] presented an analysis of transport phenomena in a proton exchange membrane fuel cell, with a focus on the modelling and assessment of non-isothermal and non-isobaric effects that have been neglected in previous studies. A model was formulated for a complete fuel cell taking into account diffusion through the porous electrodes of the humidified fuel (H_2, CO_2, and $H_2O^{(v)}$) and oxidant gases (O_2, N_2, and $H_2O^{(v)}$). The thermodynamic equilibrium potential was calculated using the Nernst equation and the reaction kinetics was determined using the Butler-Volmer equation. The model was solved numerically to analyze fuel cell performance and water transport over a range of operating current densities. Non-uniform temperature and pressure distributions were found to have a large impact on the predicted liquid water and vapour fluxes in the anode and cathode diffusion layers. In particular, the results indicated that water management requirements (i.e., humidification or water removal) to prevent potential membrane dehydration or electrode flooding were much more conservative than predicted assuming isothermal conditions.

In this work, modelling of a three-dimensional 5 kW PEMFC stack dynamic is developed. Based on this model, the dynamic response and sensitivity analyses of the stack are carried out.

Model Formulation

A schematic diagram of a typical PEM fuel cell is shown in Figure 2. The cell consists of a cathode and anode electrodes with a proton conductive membrane as the electrolyte sandwiched in between. Between each of the electrodes and the membrane there is a catalyst layer, referred to as the cathode and anode catalyst, respectively. This work is based on the models developed by Djaeni [10]. In addition, other relationships are also added to completely specify the system accurately. These include the interfacial transport equations like Butler-Volmer equation and Electrode reversible voltages, Stefan-Maxwell equation.

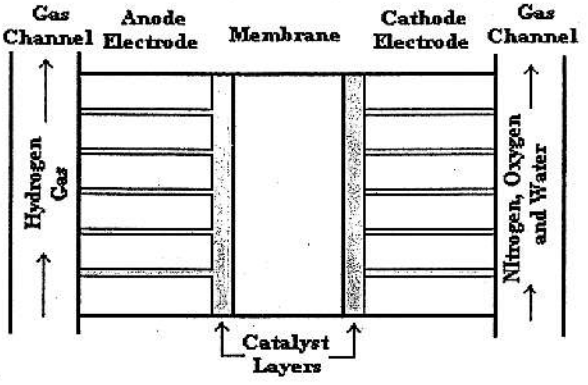

Figure 2 - A Schematic of A PEM Fuel Cell

ISBN:983-2643-15-5

Interfacial Transport Equations

The Butler – Volmer equation describes the charge transfer process across the anodic and cathodic double layer. This equation characterizes the functional relationship between the activation or charge-transfer overpotential (η) and current density for an electrode at a particular temperature, pressure and volumetric concentration of reacting species at the electrode or electrolyte interface. This equation allows the computation of the net current density flowing through an electrode or electrolyte interface for a particular overvoltage (η) established between the metallic electrode surface and the Helmholtz plane, taking into consideration the presence of a forward (i_f) and backward (i_b) current density flowing across the mentioned metal or electrolyte interface. The net current density for a one-step electrochemical reaction flowing through an electrode can be defined mathematically using the following equation:

$$i = i_f - i_b \tag{2}$$

Where the forward current density (i_f) and the backward current density (i_b) are defined as follows:

$$i_f = i_o.e^{\frac{\alpha.n.F.\eta}{R.T}} \tag{3}$$

$$i_b = i_o.e^{\frac{-(1-\alpha).n.F.\eta}{R.T}} \tag{4}$$

Consequently the expression for the net current density for one-step electrochemical reaction flowing through a metallic electrode is expressed using the following equation:

$$i = i_o.\left[e^{\frac{\alpha.n.F.\eta}{R.T}} - e^{\frac{-(1-\alpha).n.F.\eta}{R.T}}\right] \tag{5}$$

Equation (5) is called the Butler-Volmer equation. Normally the variables associated with this equation (the exchange current density i_o and the charge transfer coefficient α) are obtained from empirical procedures. This equation is considered a valid tool to explain the interfacial charge transfer process even though the detailed mechanisms of electrode electrochemical reactions are not well understood.

In addition, it is important to know that the electric potential of an isolated electrode (or absolute electric potential) cannot be measured in practice. For that reason, some relative magnitudes are defined by convention according to a specific and unequivocal scale. These magnitudes are named "electrode potentials" and are defined as the electromotive force of a cell containing the electrode under analysis and the standard hydrogen electrode (SHE), for which the voltage is arbitrarily taken as zero. Generally the reversible potential of an electrode for a specific electrochemical reaction can be separated into 3 terms. The first one represents the standard electrode potential and contains parameters that correspond to a standard state as a reference (normally 1 atm and 25 °C). The second one contains values dependant only on temperature and the third one depends directly on temperature, pressure, ion activities, etc. The following equations show the mathematically formulations for the anodic and cathodic reversible voltage.

At the anode the reversible voltage for the oxidation of pure hydrogen is given by the following equation:

$$E_r^o = \frac{\Delta G_a^o}{\alpha_a.F} - \frac{\Delta S_a^o}{\alpha_a.F}.(T - T_o) - \frac{R.T}{\alpha_a.F}.\ln(pH_2) \tag{6}$$

At the cathode the reversible voltage for the reduction of pure oxygen is given by the following equation:

$$E_r^o = \frac{\Delta G_c^o}{\alpha_c.F} - \frac{\Delta S_c^o}{\alpha_c.F}.(T - T_o) - \frac{R.T}{\alpha_c.F}.\ln(pO_2) \tag{7}$$

In a three-dimensional system the equation of mass continuity for incompressible fluid flow of constant density is expressed using the following general formula:

$$\frac{\partial \rho}{\partial t} = -\left(\frac{\partial}{\partial x}\rho.v_x + \frac{\partial}{\partial y}\rho.v_y + \frac{\partial}{\partial z}\rho.v_z\right) \tag{8}$$

Where: [14]

ρ: Fluid density, (kg/cm^3).

$\bar{v}$: Velocity vector, (cm/s).

$\rho.\bar{v}$: Mass flux, [kg/(cm^2.s)].

$\nabla.(\rho.\bar{v})$: Net rate of mass flux per unit volume, [kg/(cm^3.s)].

Rearranging terms it can be written in the following vectorial form:

$$\frac{\partial \rho}{\partial t} = -\left[\nabla.\left(\rho.\bar{v}\right)\right] \tag{9}$$

ISBN:983-2643-15-5

Equation 10 shows the Schlogl equation. In this equation, the first term is related to the electrical force acting upon the ionic species in the membrane, which is proportional to the gradient of voltage. In the second term, the parameter p represents the combined effect of static pressure and gravitational forces.

$$v = \frac{k_\phi}{\upsilon}.zf.cf.F.\nabla\phi - \frac{k_p}{\upsilon}.\nabla p \qquad (10)$$

Where:

- cf: Membrane fixed charge site concentration
- F: Faraday constant
- k_ϕ: Membrane electrokinetic permeability, (m^2).
- k_p: Membrane hydraulic permeability, (m^2).
- p: pressure, (atm).
- v: Bulk mean velocity, (m/s).
- zf: Charge of fixed (sulfonate, SO_3^-) sites,
- ϕ: Electrical potential, (V).
- υ: Pore-water viscosity, [kg/(m.s)].

The Stefan-Maxwell's equation can be considered the first step for the calculation of ordinary diffusion in multicomponent gas mixtures. If we consider the presence of an ideal gas mixture in the porous electrodes it is possible to express the mass flux in the anodic and cathodic porous electrode through the following equation:

$$J_i = \frac{c^2}{\rho}.\sum M_i.M_j.D_{ij}.\nabla.x_j \qquad i = 1,2,\ldots n \qquad (11)$$

Where:

- J_i: Mass flux of species i, [mole/(cm^2.s)].
- ρ: Fluid mass density, (kg/cm^3).
- $c = n/v = P_T/(R.T)$: Fluid molar density.
- M_i: Molar mean molecular weight of species i, (kg/mole).
- M_j: Molar mean molecular weight of species j, (kg/mole).
- D_{ij}: Diffusivity of the pair i-j in a multicomponent mixture,(cm^2/s).
- $x_j = P_i/P_T$ Mole fraction of species i, (dimensionless).

The mass flux equation 11 can be rearranged as suggested by Hart and Womack [15] to obtain the molar fraction of species 'i' using the following equation:

$$\nabla.x_i = \sum_{j=1}^{n} \frac{1}{c.D_{ij}}.\left(x_i.J_j - x_j.J_i\right) \qquad (12)$$

Equation 12 is known as the Stefan-Maxwell equation.

Energy Balance

Temperature of PEMFC is determined by the sensible heat of input and output streams, and the heat of water formation. Approximated model can be derived as:

$$\left(\frac{dT}{dt}\right) = \left(-(Q_{AN}) - (Q_{CAT}) + Q_{RFC}\right)/(Ch_{FC}) \qquad (13)$$

$$Q_{AN} = F_3\left(\int_{T_{AB}}^{T}(\sum(Cp_iC_i)dT\right. \qquad (14)$$

$$Q_{CAT} = F_A\int_{T_{AIN}}^{T}\sum(Cp_iC_i)dT \qquad (15)$$

$$Q_{HFC} = (Hf_{H2})V_{FC}(r_{H2}) \qquad (16)$$

[10]

Where:

$\left(\frac{dT}{dt}\right)_{FC}$ is the accumulation of the gases temperature leaving PEMFC (K/sec)

Q_{AN} is the heat from anode side (J/sec)

Q_{CAT} is the heat from cathode side (J/sec)

Q_{RFC} is the heat of water formation (J/sec)

Ch_{FC} is the heat capacity of PEMFC (J/K)

T is the temperature of PEMFC (K)

T_{AIN} is the temperature of inlet air (K)

Hf_{H2O} is the standard heat of water formation (J/mole)

Development of 5 kW PEM Fuel Cell Stack

The development of the fuel cell stack module models takes into considerations behaviour of individual components as well as their interactions. To simplify the development procedure, the stack is subdivided into three sub-modules. These sub-modules include power distribution, gas flow and performance.

Power Distribution

The power distribution module compares the summations of the calculated values for the single cell current and power produced to the requirement power that is 5 kW. This is done to determine if there is agreement between the

ISBN:983-2643-15-5

sum of the local values and the overall requirements. The total current produced by the k^{th} cell in the stack is calculated by summing the contributions to the total cell current that is,

$$i_k = \Sigma\, i_{cell} \qquad (17)$$

In an actual fuel cell stack the current produced by each cell is the same since they are in electrical series. Thus, it is a requirement that the calculated current produced by each cell be the same.

The total power produced by a particular cell is determined by multiplying the current for each cell by the voltage for that cell. That is,

$$P_{cell} = i_{cell} \times V_{cell} \qquad (18)$$

Finally the total power produced by the entire stack is calculated by summing the power produced by each cell in the stack. That is,

$$P_{stack} = 5\ kW = \sum_{k=1}^{K} (P_{cell})_k \qquad (19)$$

Where:

P_{stack}: Total power produced by the stack, [5 kW].

P_{cell}: Power produced by the kth cell [kW]

K: Number of cells in the stack.

Gas Flow

The gas flow module uses the flowrate information from the flowrate of a single cell. This is accomplished by first multiplying the flowrate of a single cell by the number of cells in the stack and again by the number of flow channel for each cell. This process produces the total mass flowrate of a gas at the inlet of the stack.

$$m_{x\ total} = m_{x\ inlet} \times n_c \times K \qquad (20)$$

Where:

m_x: Mass flowrate of gas x [kg/s]

n_c: Number of flow channels in a single element.

K: Number of cells in the stack.

Process Simulation

The model developed was simulated in MATLAB 6.1 environment. To model the non-steady state behaviour of a fuel stack, the modelling methodology utilised an explicit finite difference scheme. This requires the fuel cell stack to be divided into small elements. The size of each element is determined by the desired accuracy and the numerical stability of the calculations. The properties of each computational element are assumed be spatially uniform and change with time. Time is measured in discrete steps with the future state of an element calculated using the current state of the surrounding elements and material and transport properties. The size of the time steps, is also determined by the desired accuracy of the results and the numerical stability of the result; the smaller the time step, or element, the greater the accuracy and stability but the greater the number of calculations that must be completed. A numerical stable calculation is one that converges on a solution, whereas an unstable calculation does not.

After the single cell dynamic model has been developed using Matlab, the file then is converted into simulink blocks in order to develop the stack simulation that represents a 5 kW PEM fuel cell stack. The parameters and variables as well as the initial values that were necessary for simulation had been shown in Table 1 and Table 2.

Table 1 -Parameters and Variables

Parameter		Value
L	Gas channel length (m)	0.04
H	Gas channel height (m)	0.0002
W	Gas channel width (m)	0.0002
w_{diff}	Gas diffuser width (m)	0.0002
w_{cat}	Catalyst layer width (m)	3×10^{-5}
t_{mem}	Membrane thickness (m)	0.00024
α_a	Transfer coefficient, anode side	0.5
α_c	Transfer coefficient, cathode side	1
$i_{o,a}^{ref}$	Anode ref. exchange current density (A/m^2)	6×10^{-5}
$i_{o,c}^{ref}$	Cathode ref. exchange current density (A/m^2)	4.4×10^{-11}
F	Faraday constant (C/mole)	96485.31
R	Universal constant of gases (J/mole.K)	8.314
$T_{o,AB}$	Absolute reference temperature (K)	298.15
ΔG^o	Standard free energy charge (J/kmole)	2.78×10^7
ΔS^o	Standard entropy change (J/kmole)	2.86×10^8
Cf	Membrane fixed charge site concentration ($kmol/m^3$)	1.2
Zf	Fixed-site charge	-1
k_ϕ	Membrane electrokinetic permeability (m^2)	7.2×10^{-20}
k_p	Membrane hydraulic permeability (m^2)	0.20

ISBN:983-2643-15-5

υ	Pore water viscosity (kg/m.s)	$2.3x10^{-5}$
M_{H2}	Hydrogen molecular weight (kg/kmole)	2
M_{O2}	Oxygen molecular weight (kg/kmole)	32
M_{H2O}	Water molecular weight (kg/kmole)	18

Table 2 - Initial Conditions

Parameter		Value
m_{air}	Air inlet flowrates (m^3/s)	
m_{H2}	Hydrogen inlet flowrates (m^3/s)	
Ψ	Oxygen/nitrogen ratio	0.21/0.79
T	Fuel cell temperature (K)	353.15
p_c	Air side pressure (atm)	5
p_a	Fuel side pressure (atm)	3
ξ	Relative humidity of inlet gases (%)	100

Results and Discussion

This on-going works were aimed at producing complete models that completely characterizes the behaviour of the fuel cell systems. However, the focus of this paper is on the response of the feed concentrations inside the gas channel in 3-Dimensions and the overall dynamic response of the fuel cell stack. The physical properties of the membrane and electrode are the same as those given in Djaeni [10] as those given in table 1 and 2; in the discussion "base case" will be used to refer to isobaric condition.

Model validation: Isothermal and isobaric conditions

In the limit of constant pressure, the present numerical model is equivalent to the 1-D dynamic model of Djaeni [10]. In order to validate the numerical model, simulations were therefore performed first for constant gas pressure to allow comparison with the results of Djaeni. Figure 3 compares the polarization curves (voltage vs. current) computed. The results of the present model were in good overall agreement with Djaeni's data; the slight difference between the two can be attributed to the different treatments of the gas channel and anode: in the present model (i) the gas channel are considered, and (ii) the anode diffusion layer is included.

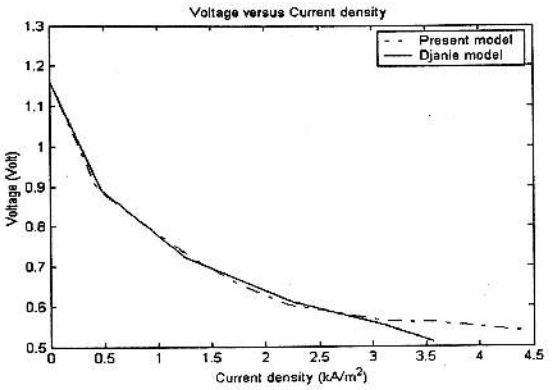

Figure 4 - Comparison of Predicted Isobaric Performance Curves With the Model of Djaeni [10]

Behaviour of feeds concentration in the gas channel

The present model considered only three species in the gas channels; hydrogen in the anode channel and in the cathode channel, oxygen and water. The distributions of the feed species are presented in figure 4 and 5 and the run time is 100 second.

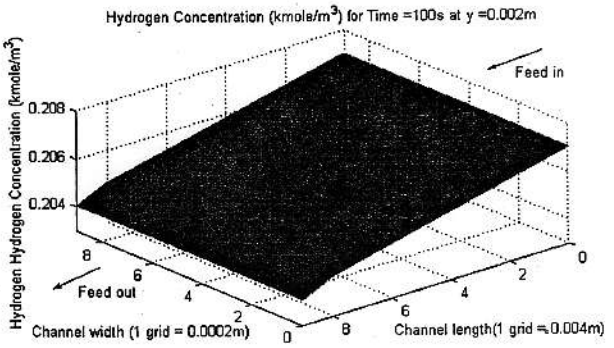

Figure 4 - Hydrogen Concentration Distribution in the Anode Gas Channel.

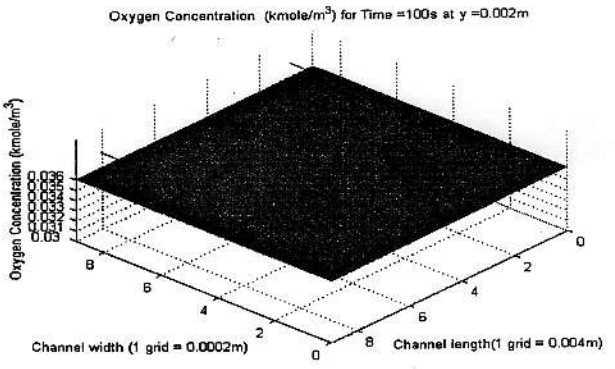

Figure 5 - Oxygen Concentration Distribution in the Cathode Gas Channel.

The hydrogen and oxygen concentrations as illustrated in figure 4 and 5 decrease from 0.20705 kmole/m^3 to 0.20405 kmole/m^3 and from 0.036231 kmole/m^3 to 0.036044

ISBN:983-2643-15-5

kmole/m^3 respectively. The concentrations drop along the channels because the reactants are diffused to the electrode region (gas diffusion layers). The diffusion process is a continued until the concentrations between the two regions are equal.

Stack Temperature

Figure 7 shows the stack temperature generated from the energy balance equations using ODE solver. The temperature of the stack is 328.15 K after 35 second simulated.

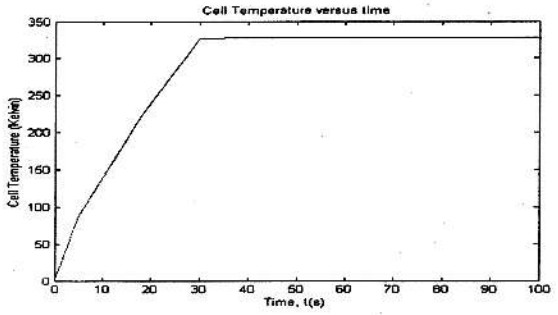

Figure 7 - The Temperature of the PEMFC Stack.

Dynamic response analysis

Figure 8 shows the schematic diagram of input-output of the PEMFC. In this system, the effect of hydrogen flow on the power is observed. The flow of hydrogen is changed and air is adjusted at constant flow. Figure 9 presents the results of the procedure.

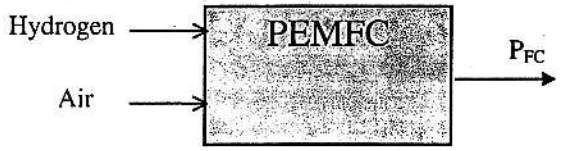

Figure 8 - The Schematic Diagram of The Input-Output of PEMFC stack

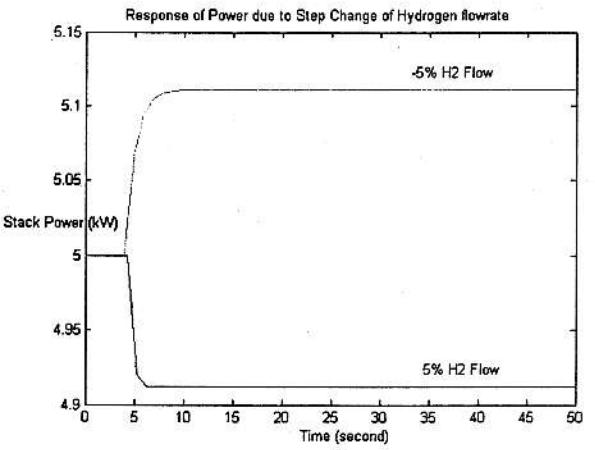

Figure 9 - Response of P_{FC} Due to The Step Change of F_H

Figure 9 shows the response of the cell power output to step change of hydrogen flow. In this case, the produced power decreases with the increase of hydrogen flow. This is because; the increase of hydrogen flow decreases the residence time. Consequently, the ionization of the hydrogen at the anode also drops because of the shorter contact time. Besides, the increase of hydrogen flow reduces the temperature of PEMFC, since temperature of hydrogen fed into the system is lower than the operating temperature of PEMFC. As a result, the reaction rate of water formation or electric current generation became slower.

Conclusion

The models for a single cell and 5 kW PEM fuel cell stack have been developed in this study. The single cell model includes 3-D feeds concentration distribution in the channels and polarization curves indicate the behaviours of the voltage and current density produced. The model was simulated in MATLAB 6.1 environment. The 5 kW PEM fuel cell stack model includes the stack temperature and power. The model was simulated in SimuLink and analyses of the dynamic behaviour of the process were carried out. Results are in agreement to the work of Djaeni [10].

Acknowledgements

This work is funded by the Ministry of Science, Technology and the Environment through National Science Foundation Scholarships and IRPA research grant. Our heartiest appreciations are for everybody who has directly or indirectly contribute to the success of this project.

References

[1] Springer, T. E., and Zawodzinski, T. A. 1991. Polymer Electrolyte Fuel Cell Model. *Journal of the Electrochemical Society*. Vol 138, No. 8. 2334.

[2] Srinivasan, S., Velev, O. A., Parthasarathy, A., Mando, D. J. and Appleby, A. J. 1991. High Energy

ISBN:983-2643-15-5

Efficiency and High Power Density Proton Exchange Membrane Fuel Cells – Electrode Kinetics and Mass Transport. *Journal of Power Sources*. 36. 299-320.

[3] Amplett, J. C., Baumert, R. M., Mann, R. F., Peppley, B. A., and Roberge, P. R., 1995. Performance Modelling of the Ballard Mark IV Solid Polymer Electrolyte Fuel Cell, I. Mechanistic Model Development. *Journal of Electrochemistry Society*. 142, No. 1. 1-8.

[4] Amplett, J. C., Baumert, R. M., Mann, R. F., Peppley, B. A., and Roberge, P. R., 1995a. Performance Modelling of the Ballard Mark IV Solid Polymer Electrolyte Fuel Cell, II. Empirical Model Development. *Journal of Electrochemistry Society*. 142, No. 1. 9-15.

[5] West, A.C. and T.F. Fuller 1996. Influence of Rib Spacing in Proton-Exchange Membrane Electrode Assemblies. *Journal of Applied Electrochemistry*. 26. 557-565

[6] Lee, J. H., Lalk, T. R., and Appleby, A. J. 1998. Modelling Electrochemical Performance In Large Scale Proton Exchange Membrane Fuel Cell Stacks. *Journal of Power Sources*. 70. 258-268.

[7] Lee, J. H. and Lalk, T. R. 1998a. Modelling Fuel Cell Stack Systems. *Journal of Power Sources*. 73. 229-241.

[8] Gurau, V., Liu, H. and Kakac, S. 1998. Two Dimensional Model For Proton Exchange Membrane Fuel Cells. *Journal of AIChE*. 44. 2410-2422

[9] Kulikovsky, A., Divisek, J. and Kornyshev, A. 1999. Modelling the Cathode Compartment of Polymer Electrolyte Fuel Cells: Dead and Active Reaction Zones. *Journal of Electrochemical Society*. 146. 3981-3991.

[10] Djaeni, M 1999. Modelling and Control of Fuel Cell System. Msc. Diss., Universiti Teknologi Malaysia:

[11] Mann, R. F., Amphlett, J. C., Hopper, M. A. I., Jensen, H. M., Peppley, B. A. and Roberge, P. R. 2000. Development and Application of A Generalised Steady-State Electrochemical Model For A PEM Fuel Cell. *Journal of Power Sources*. 86. 173-180.

[12] Rowe, A. and Li, X. 2001. Mathematical Modelling of Proton Exchange Membrane Fuel Cells. *Journal of Power Sources*. 102. 82-96.

[13] Djilali,N. and Lu,D. 2002. Influence of Heat Transfer On Gas and Water Transport In Fuel Cells. *International Journal of Thermal Sciences*. 41. 29-40.

[14] Hirchenhofer, J. H., Stauffer, D. B., Engleman, R. R. and Klett, M. G. 1998. *Fuel Cell Handbook*. Fourth Edition. DOE/FETC-99/1076.

[15] Hart, A.B. and G.J. Womack 1967. *Fuel Cell Theory and Application*. Chapman and Hall Ltd., London

ISBN:983-2643-15-5